Plasma waveguide array induced by filament interaction

Xuan Yang, Jian Wu, Yan Peng, Yuqi Tong, Peifen Lu, Liang'en Ding, Zhizhan Xu, and Heping Zeng*

State Key Laboratory of Precision Spectroscopy, East China Normal University, Shanghai 200062, China
**Corresponding author: hpzeng@phy.ecnu.edu.cn*

Received August 27, 2009; revised October 4, 2009; accepted October 16, 2009;
posted October 27, 2009 (Doc. ID 116194); published December 7, 2009

We demonstrate that interference-assisted coalescence of two noncollinearly overlapped filaments creates a wavelength-scale periodic plasma density modulation to guide the input pulses equivalently as a photonic crystal plasma waveguide. The periodic self-channeling is evidenced by the direct observation of the filament coalescence, which reveals wavelength-scale spatial widths and periodicity dependent on the crossing angles and intensity ratios between the incident filaments. © 2009 Optical Society of America

OCIS codes: 230.7380, 320.7110, 190.4360.

Intense ultrashort pulses propagating in neutral media undergo filamentation with self-stabilized intensity clamping in self-guided channels [1] owing to the counterbalance between Kerr self-focusing and plasma defocusing, which mediate abundant self-action and cross-coupling nonlinearities, such as spatial self-cleaning [2], supercontinuum generation [3], pulse self-compression [4], and terahertz emission [5]. Multifilamentation typically occurs for quite high-intensity pulses, and coalescence of multiple filaments cannot increase the tightly guided peak intensity beyond the clamping limit. Recently, ever-growing experimental explorations of the interaction of multiple filaments have already revealed quite a lot of intriguing features of light-bullet fusion [6], fission [7], and spiraling [8] as a stimulus to potential applications with nonlinearly coupled multiple filaments instead of a single filament.

Here we demonstrate that spatial grating established by interfering two noncollinearly overlapped intense femtosecond beams could assist coalescence of the incident filaments into a lattice of strongly coupled parallel self-channels with wavelength-scale structure in the intersection as 1D photonic crystal filaments. It is well known that nonlinear interference of noncollinear beams could establish transient holographic gratings by virtue of nonlinear changes of the refractive index within a limited interaction length that induce nonlinear diffraction rather than tightly guiding. A periodic lattice of microstructures could be created by recording the interference pattern in photosensitive media [9], typically applicable to guide low-intensity beams. The full potential of photonic crystal waveguides could be maximized to guide high-intensity pulses over long lengths in gases by creating a wavelength-scale periodic plasma density modulation.

As two slightly focused noncollinear femtosecond pulses are synchronized near the overlapped foci, their constructive and destructive interference produces a periodic local intensity distribution, and wavelength-scale self-channels are created by the dynamic interplay between several mechanisms. First, Kerr self-focusing is launched for the constructive interference peaks, resulting in a further increase of the local peak intensity. Second, this process is balanced in the corresponding localized regions by multiphoton-ionization-induced plasma defocusing and higher-order terms of the nonlinear refractive index. As a whole, noncollinear interference facilitates a periodic plasma density modulation to guide the input pulses into 1D photonic crystal filaments in air.

The experiment used a Ti:sapphire laser (1 kHz, 800 nm, 50 fs, 2.0 mJ), which was equally split into two parts as the pump and probe beams. The split pulses were slightly focused with two high-reflection concave mirrors (f=100 cm) and crossed at an angle variable from 2° to 16°. Two noncollinear filaments (50 mm) were generated when they were temporally separated [Fig. 1(a)]. As two noncollinear pulses of the same polarizations were synchronized, interaction was observed, as shown in Fig. 1(c). Their constructive and destructive interference induced a spatial intensity modulation and produced a periodic local intensity distribution along the crossing plane. We monitored the intensity distributions of optical

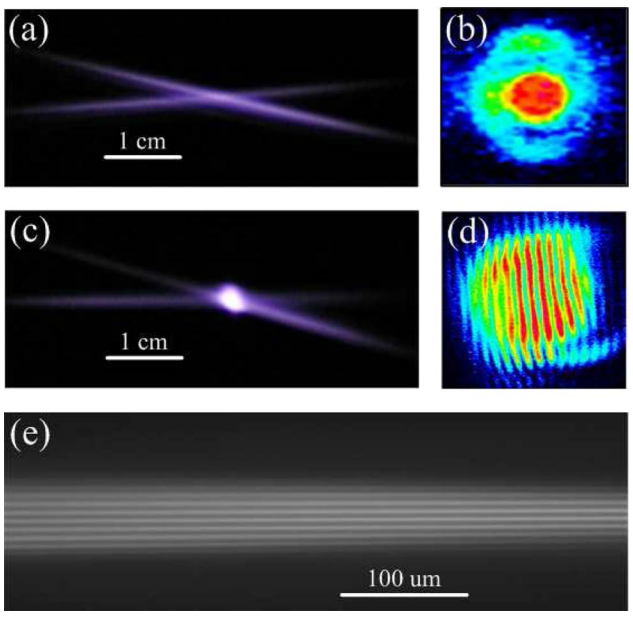

Fig. 1. (Color online) (a), (c) Top view and (b), (d) transversal distribution of the overlapped noncollinear filaments for the cases without and with filament interaction. (e) Measured N_2 fluorescence profile of the interacting region.

 © 2009 Optical Society of America

fields in the interaction region by inserting a thin plate (1 cm before the foci) at a grazing angle to reflect part of the crossing beams, and we recorded the reflected beams with an intensified CCD after an imaging system. No intensity modulation was observed when the incident filaments were temporally delayed far away [Fig. 1(b)], while distinct intensity modulation was observed for synchronized crossing filaments [Fig. 1(d)]. Interestingly, the filament fluorescence generated by the N_2 molecules in the plasma increased significantly in the overlapping region. We measured the fluorescence with an optical imaging system consisting of a UV CCD and a 10× microscope objective [10]. A bandpass filter (from 250 to 380 nm) was used to select only the blue and UV nitrogen fluorescence from the neutrals and from the excited ions. As shown in Fig. 1(e), periodic nitrogen fluorescence distribution appeared in the overlapped region, which justified the existence of refractive index modulation from the plasma (ions).

Each individual filament without filament interactions was accompanied by spatial self-cleaning in the core [2] with a significant improvement of the spatial distribution in the far-field region, as shown in Fig. 2(a). We imaged the expanding beams on a white paper screen placed 1.5 m after the beam crossing with a camera. For synchronized pump and control pulses, bowlike diffraction of each filament and threadlike fringes between the two filaments were observed in the far-field region, as shown in Fig. 2(b). The bowlike diffraction whose spectrum ranged from 650 to 830 nm was caused by the self-phase and cross-phase modulations, suggesting strong spatiotemporal couplings in the interaction region, while the threadlike fringes whose spectrum ranged from 775 to 825 nm indicated self-guiding in the 1D photonic crystal filaments. Note that these threadlike fringes were not caused by diffraction from the filament, since diffraction should be accompanied by diffraction patterns with bright and energy-concentration spots in the centers to represent the incident beam distributions. However, no bright and energy-concentration spots were observed in the threadlike fringes, excluding their origin from diffraction. Owing to nonlinear coupling of filament in the overlapping region, the intensity was spatially modulated, and the refractive index was redistributed, leading to an increase or decrease of the local refractive index. Accordingly, the incident pulses changed their original propagation directions, were confined in the high-refractive-index region, and were further self-guided in the 1D photonic crystal filaments and projected in the far-field region as threadlike fringes. A holograph technique [11] was used to measure the time evolution of 1D photonic crystal filaments. Here, we used a third weak beam with controllable time delays to perpendicularly propagate through the interaction region (from the bottom to the top). The image was optically magnified by a factor of $M=f_2/f_1$ in a $4f$ configuration with lenses L1 and L2 of focal lengths $f_1=40$ cm and $f_2=200$ cm, respectively. A CCD camera (1260 × 1024 pixels, 6.7 mm pixel size) was placed at the image plane to capture a magnified image. The images of 1D photonic crystal filaments at different time delays (1.0, 3.0, and 5.0 ps) are shown in Figs. 2(d)–2(f). This indicates that the 1D photonic crystal filaments were related to the plasma grating, which continued to exist after the passage of the two synchronized pulses. Figure 2(c) depicts the averaged intensity profile of the threadlike fringes recorded by the CCD in the far-field region. The measured energy ratio between the threadlike fringes and nondeviated beams was 1:50, which indicated an energy coupling efficiency of 2% into the 1D photonic crystal filaments.

The filament coalescence was further confirmed by measuring the N_2 fluorescence with the optical system mentioned above, which provided a direct observation of the filament interaction zone in the incident plane. As is clearly shown in Fig. 3(a), the surrounding energies were attracted to interaction region near the interference peaks [12]. Interestingly, such regular interference patterns started even when the individual filaments were separated without observable

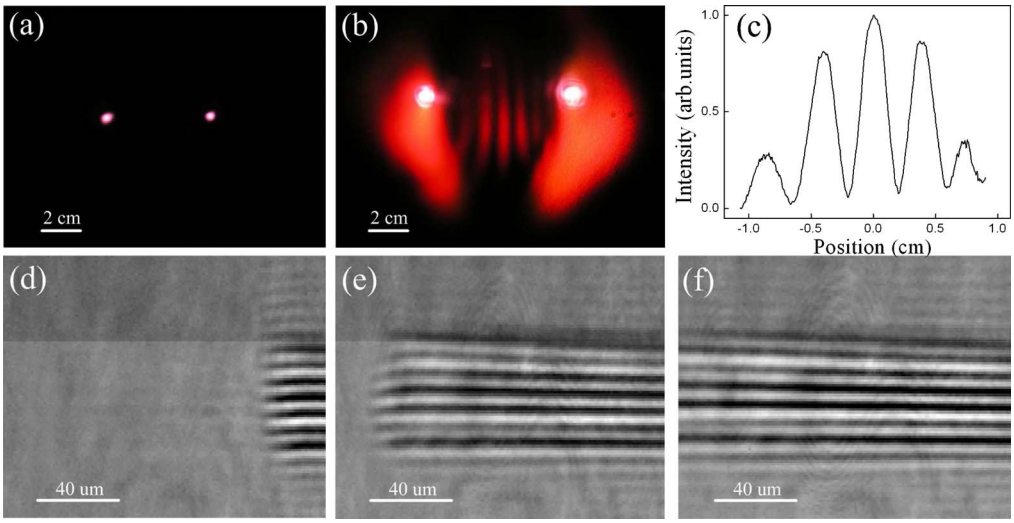

Fig. 2. (Color online) Far-field image of the beam profiles (a) without and (b) with interaction. (c) Averaged fringe intensity profiles appearing between the two filaments for (b). 1D photonic crystal filaments at different time delays of (d) 1.0, (e) 3.0, and (f) 5.0 ps.

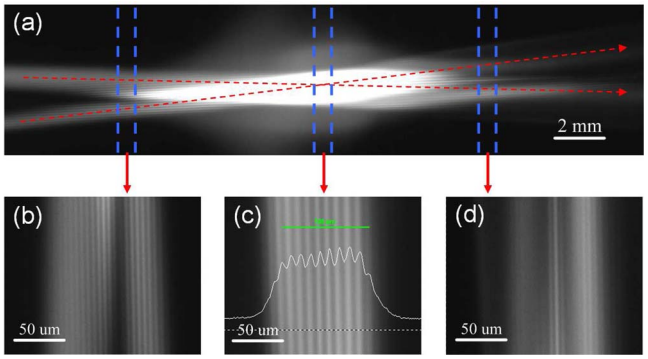

Fig. 3. (Color online) (a) Measured fluorescence profile of the interacting filaments with (b)–(d) detailed transversal fringes at different propagation distances.

spatial overlapping, as shown in Fig. 3(b). This took place as the pump (probe) pulses interfered with the spatial peripheries of the probe (pump) pulses and thus created slight but regular spatial intensity modulations. The input pulses were eventually guided into photonic crystal filaments, as shown in Fig. 3(c). And as shown in Fig. 3(d), the incident pulses were partly guided along the bisector of the noncollinearly overlapped filaments, consistent with the observed filament profiles in the far-field region [Fig. 2(b)].

As the plasma density modulation exhibited a spatial periodicity determined by the pump and probe wave vectors, both pump and probe pulses at large incident angles could be coupled into the 1D photonic crystal filaments [Figs. 3(a) and 3(b)] because of the automatic balance between the incident beam wave vectors and plasma grating periodicity. The 1D photonic crystal filaments encountered fission into individual filaments [Fig. 3(d)] owing to energy loss from the multiphoton ionization that broke the counterbalance in self-focusing and plasma defocusing after a few millimeters of propagation. As a whole, filament coalescence and fission of 1D photonic crystal filaments were interconnected by tight confinement in the 1D photonic crystal filaments, equivalent to nonlinear couplers for high-peak-intensity pulses.

As the formation of photonic crystal filaments was based on the filament interference, the widths and numbers of self-channels were determined by the interference period given by $\lambda/[2\sin(\alpha/2)]$. Figure 4 shows the observed photonic crystal filaments at different crossing angles between the two filaments. As the crossing angle increased, the self-channel width decreased with increased self-channel number in the overlapped region. The self-channel widths at crossing angles α=3°, 5°, 7°, and 14° were, respectively, measured to be 7.9, 5.2, 3.8, and 1.4 μm, which agreed with the theoretical calculated values of 7.7, 4.6, 3.3 and 1.6 μm based on the interference period.

In summary, we have experimentally demonstrated the formation of wavelength-scale periodic arrays of self-guided channels in air by using the interaction of noncollinearly overlapped intense filaments, which opens an avenue to control filament interactions and filamentation nonlinear optics. The

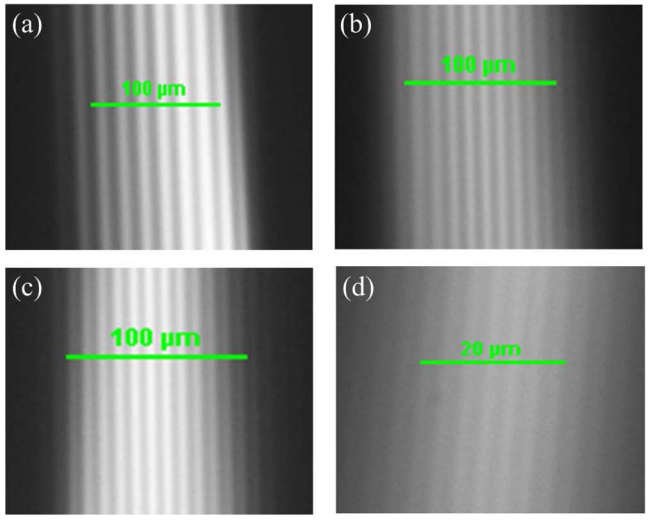

Fig. 4. (Color online) Measured distribution of the 1D photonic crystal filaments at crossing angles of (a) 3°, (b) 5°, (c) 7°, and (d) 14°.

self-guided channels with wavelength-scale periodic array structures may stimulate interesting applications in high-intensity optics and lattice solitons [13].

This work was funded by National Natural Science Fund (10990101, 10525416, and 10804032), and National Key Project for Basic Research (2006CB806005). Z. Xu also works at State Key Laboratory for High Intensity Optics, Shanghai Institute of Optics and Fine Mechanics, Chinese Academy of Sciences, Shanghai 201800, China.

References

1. A. Couairon and A. Mysyrowicz, Phys. Rep. **441**, 47 (2007).
2. F. Théberge, N. Aközbek, W. W. Liu, A. Becker, and S. L. Chin, Phys. Rev. Lett. **97**, 023904 (2006).
3. J. Yu, D. Mondelain, G. Ange, R. Volk, S. Niedermeier, J. P. Wolf, J. Kasparian, and R. Sauerbrey, Opt. Lett. **26**, 533 (2001).
4. A. Couairon, M. Franco, A. Mysyrowicz, J. Biegert, and U. Keller, Opt. Lett. **30**, 2657 (2005).
5. S. Tzortzakis, G. Méchain, G. Patalano, Y.-B. André, B. Prade, M. Franco, A. Mysyrowicz, J.-M. Munier, M. Gheudin, G. Beaudin, and P. Encrenaz, Opt. Lett. **27**, 1944 (2002).
6. V. Tikhonenko, J. Christou, and B. Luther-Davies, Phys. Rev. Lett. **76**, 2698 (1996).
7. W. Krolikowski and S. Holmstrom, Opt. Lett. **22**, 369 (1997).
8. M.-F. Shih, M. Segev, and G. Salamo, Phys. Rev. Lett. **78**, 2551 (1997).
9. J. W. Fleischer, M. Segev, N. K. Efremidis, and D. N. Christodoulides, Nature **422**, 147 (2003).
10. H. L. Xu, A. Azarm, J. Bernhardt, Y. Kamali, and S. L. Chin, Chem. Phys. **360**, 171 (2009).
11. M. Centuriona, Y. Pu, and D. Psaltis, J. Appl. Phys. **100**, 063104 (2006).
12. S. A. Hosseini, Q. Luo, B. Ferland, W. Liu, S. L. Chin, O. G. Kosareva, N. A. Panov, N. Aközbek, and V. P. Kandidov, Phys. Rev. A **70**, 033802 (2004).
13. D. N. Christodoulides and R. I. Joseph, Opt. Lett. **13**, 794 (1988).